

A New Calculation of the NLO Energy-Energy Correlation Function

G. Kramer^a, H. Spiesberger^b

^aII. Institut für Theoretische Physik^{*,†}

Universität Hamburg

D - 22761 Hamburg, Germany

^bDeutsches Elektronen-Synchrotron DESY

D - 22603 Hamburg, Germany

Abstract

We present a new calculation of the $O(\alpha_s^2)$ coefficient of the energy-energy correlation function (EEC) using two different schemes to cancel infrared and collinear poles. The numerical evaluation uses the phase space slicing and the hybrid subtraction method. Both schemes converge with decreasing slicing cut. The results are independent of the scheme for small cuts. For the pure phase space slicing method, the cut must be below 10^{-6} to achieve good results. All four approaches agree with each other and confirm the results of Kunszt and Nason and Glover and Sutton, for the latter also with respect to contributions of different colour factors.

* Supported by Bundesministerium für Forschung und Technologie, Bonn, Germany, Contract 05 6HH93P(5).

† Supported by the EEC Program 'Human Capital and Mobility' through Network 'Physics at High Energy Colliders' under Contract CHRX-CT93-0357 (DG12 COMA).

1 Introduction

The energy-energy correlation function Σ has been used by all for LEP experiments [1] and the SLD experiment [2] at SLAC to measure the strong coupling constant α_s in e^+e^- annihilation at the Z resonance. Σ is defined as a function of the angle χ between two particles i and j in the following form

$$\frac{d\Sigma(\chi)}{d\cos\chi} = \frac{\sigma}{\Delta\cos\chi N_{event}} \sum_{N_{event}} \sum_{i \neq j} \frac{E_i E_j}{E^2} \quad (1)$$

where E_i and E_j are the energies of the particles and E is the total energy of the event, $E^2 = s$. The sum runs over all pairs i, j with $\cos\chi$ in a bin of width $\Delta\cos\chi$: $\cos\chi - \Delta\cos\chi/2 < \cos\chi < \cos\chi + \Delta\cos\chi/2$. Each pair enters twice in the sum. The limits $\Delta\cos\chi \rightarrow 0$ and $N_{event} \rightarrow \infty$ have to be taken in (1). σ is the total cross section for $e^+e^- \rightarrow hadrons$.

In perturbative QCD the energy-energy correlation function (EEC) is given as a series in α_s which we write as

$$\frac{1}{\sigma_0} \frac{d\Sigma}{d\cos\chi} = \frac{\alpha_s(\mu)}{2\pi} A(\chi) + \left(\frac{\alpha_s(\mu)}{2\pi} \right)^2 \left(\beta_0 \ln\left(\frac{\mu}{E}\right) A(\chi) + B(\chi) \right) + O(\alpha_s^3), \quad (2)$$

where $\beta_0 = (11N_c - 4T_R)/3$. For QCD we have $C_F = 4/3$, $N_C = 3$ and $T_R = N_f/2$ where N_f is the number of active flavours at energy E .

The first order term $A(\chi)$ is calculated from the well-known one-gluon emission diagrams $\gamma^*, Z \rightarrow q\bar{q}g$, where χ is the angle between any of the three partons. It has been first calculated by Basham et al. [3] with the result

$$A(\chi) = C_F(1 + \omega)^3 \frac{1 + 3\omega}{4\omega} \left((2 - 6\omega^2) \ln(1 + 1/\omega) + 6\omega - 3 \right) \quad (3)$$

where $\omega = \cot^2 \chi/2$. The next-to-leading order (NLO) contribution $B(\chi)$ is obtained from the processes $\gamma^*, Z \rightarrow q\bar{q}g$ at one loop and $\gamma^*, Z \rightarrow q\bar{q}gg, q\bar{q}q\bar{q}$ at tree level. Several groups have calculated $B(\chi)$ in the past: Richards, Stirling and Ellis (RSE) [4], Ali and Barreiro (AB) [5], Schneider, Kramer and Schierholz (SKS) [6], Falck and Kramer (FK) [7], Kunszt and Nason (KN) [8], Glover and Sutton (GS) [9] and just recently Clay and Ellis (CE) [10]. Most of the calculations, except those of SKS and FK, are based on the ERT matrix elements [11]. The numerical evaluations differ by the method used to cancel infrared and collinear divergences.

Considering the results for $B(\chi)$ obtained by RSE, AB, FK and KN one notices that they differ at the special point $\chi = \pi/2$ by roughly 50%. The SLD collaboration [2] used all four theoretical calculations to determine α_s from their measurements. They averaged the values of α_s obtained this way and increased the theoretical error accordingly. This additional error of α_s due to the uncertainty over which the coefficient $B(\chi)$ in the EEC is correct is equal to ± 0.006 , which is appreciable, considering that the pure experimental error is only $(+0.002, -0.003)$ and the error from the hadronisation corrections is ± 0.002 . This unsatisfactory situation has raised renewed interest in the calculation of the EEC function and Glover and Sutton [9] have presented a new calculation of $B(\chi)$ using three methods, called subtraction, phase space slicing and hybrid subtraction method. They confirmed the result of Kunszt and Nason [8]. In the most recent calculation of Clay and Ellis [10] a larger value of $B(\chi)$ is obtained which agrees

with the result of Falck and Kramer [7], but is in disagreement with the other recent calculations of GS and KN. CE argued, on the basis of their much higher statistical precision of $\pm 0.3\%$, that the theoretical error on α_s could be reduced now; however, this does not seem justified since the spread of theoretical predictions did not change with this new calculation. One might think, that the theoretical prediction of the $O(\alpha_s^2)$ coefficient $B(\chi)$ should be unique with no other uncertainty than the error of the numerical evaluation. However, we will see later that this need not always be the case.

In order to compute the NLO term $B(\chi)$ in (2) it is necessary to combine the contribution from the 3-parton one-loop diagrams (multiplied with the LO graphs) with the 4-parton $\gamma^*, Z \rightarrow q\bar{q}gg, q\bar{q}q\bar{q}$ processes. The virtual matrix elements contain infrared and collinear singularities which cancel with the singularities in the matrix elements of the 4-parton final state. This cancellation of the infrared and collinear poles is done analytically using dimensional regularisation. The extraction of the infrared and collinear poles in the regulator ϵ (dimension $n = 4 - 2\epsilon$) and the complete calculation of the finite terms for $\epsilon \rightarrow 0$ has been done by two groups independently with identical results [11, 13]. An analytical calculation of the full 4-parton expressions at finite ϵ is not possible. Therefore these expressions are simplified in such a way that they contain all the infrared and collinear singularities. Analytical integrals of these simplified 4-parton matrix elements were then added to the virtual 3-parton contributions and the sum was shown to be finite in the limit $\epsilon \rightarrow 0$. The difference between the exact 4-parton matrix elements and the simplified expressions was then computed in 4 dimensions using numerical methods. To calculate this difference, essentially two methods have been applied which are denoted subtraction and phase space slicing method in the literature [14]. These two methods can nicely be explained following Kunszt and Soper [14] by considering a simple one-dimensional integral

$$T = \lim_{\epsilon \rightarrow 0} \left(\int_0^1 \frac{dx}{x} x^\epsilon F(x) - \frac{1}{\epsilon} F(0) \right) \quad (4)$$

where $F(x)$ is a known function representing the 4-parton matrix elements. x is the variable which produces the singularity, i.e. it is the energy of the gluon, the angle of two partons or an invariant mass which approaches zero in the infrared or collinear limit. The integration over x represents the additional phase space of the parton which produces the pole term. The integrand is regularized by the factor x^ϵ as it appears in dimensional regularization. The first term is still divergent for $\epsilon \rightarrow 0$. So to cancel the divergence of the second term, which represents the divergent contribution from loop diagrams for the 3-parton matrix elements, one must do the integral for $\epsilon \neq 0$. Now the two methods to perform this integration are as follows. First in both methods one isolates the singularity of the integrand by subtracting the pure pole term $F(0)/x$ and adding it to the second term with the result

$$\begin{aligned} T &= \lim_{\epsilon \rightarrow 0} \left(\int_0^1 \frac{dx}{x} x^\epsilon (F(x) - F(0)) + F(0) \int_0^1 \frac{dx}{x} x^\epsilon - \frac{1}{\epsilon} F(0) \right) \\ &= \int_0^1 \frac{dx}{x} (F(x) - F(0)) \end{aligned} \quad (5)$$

This way the infrared singularity is cancelled and one is left with a manifestly finite integral which is evaluated at $\epsilon = 0$. Due to the complicated structure of the 4-parton matrix elements this last integral must be calculated numerically. The above procedure defines the subtraction method and was first used for the calculation of event shape distributions in e^+e^- annihilation

by Ellis, Ross and Terrano [11].

An alternative approach is the phase space slicing method which is familiar from many QED calculations. It was first applied in a NLO calculation of the thrust distribution in e^+e^- annihilation by Fabricius, Schmidt, Schierholz and Kramer [15]. In this method the integration region in (4) is divided into two parts, $0 < x < y_{min}$ and $y_{min} < x < 1$. In the first region, the function $F(x)$ can be approximated by $F(0)$ provided the arbitrary slicing parameter $y_{min} \ll 1$, so that

$$\begin{aligned} T &= \lim_{\epsilon \rightarrow 0} \left(\int_{y_{min}}^1 \frac{dx}{x} x^\epsilon F(x) + \int_0^{y_{min}} \frac{dx}{x} x^\epsilon (F(x) - F(0)) + F(0) \int_0^{y_{min}} \frac{dx}{x} x^\epsilon - \frac{1}{\epsilon} F(0) \right) \\ &= \int_{y_{min}}^1 \frac{dx}{x} F(x) + \int_0^{y_{min}} \frac{dx}{x} (F(x) - F(0)) + F(0) \ln y_{min} \\ &\simeq \int_{y_{min}}^1 \frac{dx}{x} F(x) + F(0) \ln y_{min}. \end{aligned} \quad (6)$$

The last equation in (67) follows when $y_{min} \ll 1$ is chosen small enough, so that the finite integral

$$T_f = \int_0^{y_{min}} \frac{dx}{x} (F(x) - F(0)) \quad (7)$$

can be neglected. If this is the case the integral T should not depend on y_{min} which usually is taken as evidence that T_f is indeed negligible. This cutoff dependence was investigated, for example, for the thrust distribution in [16] and for y_{min} small enough ($y_{min} \leq 10^{-4}$, where y_{min} was the invariant mass cutoff) the result was found to agree with the thrust distribution obtained with the subtraction method [17, 18]. It is clear that if the finite contribution T_f in (7) is not neglected both the subtraction and the phase space slicing method must give the same results, independent of how small the cutoff y_{min} is. If the finite term is kept, we have for T

$$T = \int_{y_{min}}^1 \frac{dx}{x} F(x) + F(0) \ln y_{min} + T_f. \quad (8)$$

This version is called the hybrid subtraction method in the recent work of Glover and Sutton [9] and will be called the hybrid method in the following.

It is clear that in this simple example, the results for T in the subtraction method and in the hybrid method are identical, independent of how y_{min} has been chosen in (8). However, in the actual application to the EEC the situation is more complicated. In this case the function " $F(x)/x$ " is the matrix element of the process $e^+e^- \rightarrow 4 \text{ partons}$ which depends on five variables, whereas " $F(0)$ " corresponds to a contribution to the 3-parton final state, $e^+e^- \rightarrow 3 \text{ partons}$, which depends only on two variables. Both contributions have to be integrated out up to the one variable $\cos \chi$ and in order to complete the definition of the EEC function one has to supply a prescription for the calculation of $\cos \chi$. In the region $x \geq y_{min}$ where x stands for one of the variables for which the matrix elements become singular, it is most natural to determine $\cos \chi$ from the pairing of two of the 4 parton momenta p_1, p_2, p_3 and p_4 , i.e.

$$\cos \chi = \hat{\vec{p}}_i \hat{\vec{p}}_j \quad (9)$$

with $i, j = 1, \dots, 4$. The finite integral T_f in (7) can be calculated at least in two ways: (i) the integrand " $F(x)/x$ " is calculated with 4-parton kinematics, i.e. with (9) and $i, j = 1, \dots, 4$, whereas the subtracted integrand " $F(0)/x$ " is calculated with variables corresponding to 3 partons in the final state, i.e. with (9) and $i, j = 1, \dots, 3$, of course after the integration over x and two more variables is performed in the 4-parton case; (ii) the whole integral with integrand $(F(x) - F(0))/x$ is evaluated with 3-parton kinematics. The latter procedure amounts to performing the integration over x and two more of the 4-parton variables with two variables considered constant which are then identified with the two variables describing a 3-parton final state. With other words, for the evaluation of T_f one has the freedom to treat the contribution $F(x)/x$ exactly or with recombination of two of the partons into one jet. The selection of the partons i, j , which are recombined is determined by that one of the variables $y_{ij} = (p_i + p_j)^2/s$ which leads to the singularity and which is identified with x in the example integral. It is clear that this recombination procedure is not unique and we shall consider two possibilities later on. In the limit $y_{min} \rightarrow 0$ the distinction (i) and (ii) should not matter. But for finite $y_{min} > 0$ we expect a difference between (i) and (ii). The procedure (i) is used in the subtraction approach, so that for (i) the result of the hybrid method should be independent of y_{min} whereas with (ii) the region where the recombination is performed is changed so that we expect that the total integral will depend on y_{min} . The y_{min} dependence should be smaller than in the phase space slicing approach, in which the integral T_f is neglected altogether. It is the general consensus that all these methods should give legitimate results, provided y_{min} is chosen small enough.

As in previous work we focus on the zero-resolution limit ($y_{min} \rightarrow 0$), i.e. we do not apply a recombination procedure to all of the two-parton combinations to form jets before the calculation of the EEC function is done. Calculations with a jet recombination for all possible parton pairings were performed by AB [5] and by SKS [6] using Sterman-Weinberg (ϵ, δ) cuts and also in a recent experimental analysis of the ALEPH collaboration [19].

To shed some further light on the question where the discrepancy between the various calculations could arise we have made the effort to perform a new calculation of $B(\chi)$ using the hybrid method in the form (ii) described above. In recent work [20] we have studied the asymptotic behaviour of $B(\chi)$ for $\chi \rightarrow \pi$ in order to compare with the predictions of the leading logarithm approximation for large angles [21] using the hybrid method in the same form. Here we extend these calculations to the whole χ range. In addition, we separated the contributions of the different phase space regions, which can be characterized by the first, second and third term in (8) for the example integral. Furthermore to explore the source of the discrepancies we decompose $B(\chi)$ into the contributions from different colour factors

$$B(\chi) = C_F^2 B_{C_F}(\chi) + C_F N_C B_{N_C}(\chi) + C_F N_f B_{N_f}(\chi) \quad (10)$$

which can be compared with the results of other calculations. In section 2 we describe the two methods used to calculate the $O(\alpha_s^2)$ contribution to the EEC and present the results for the various colour factors separated according to the different phase space regions. In section 3 we compare our results with the earlier calculations and comment on the different approaches. We end with some concluding remarks.

2 Calculational Methods and Results

The new calculation of the EEC in $O(\alpha_s^2)$ is based on the approach described in detail in [22]. It starts from known $O(\alpha_s^2)$ matrix elements for $e^+e^- \rightarrow 3 \text{ partons}$ [11, 13] and $e^+e^- \rightarrow 4 \text{ partons}$ [23, 11]. To obtain finite results, in which all infrared and collinear singularities are cancelled we introduce a phase space slicing cut to separate the 4-parton phase space from the region in which the integration over one of the invariants y_{ij} producing the singularity has been done analytically in n dimensions. This integration region is defined by

$$y_{ij} = (p_i + p_j)^2/s < y_{min} \quad (11)$$

where y_{min} is the parameter to separate the two regions and i, j are the labels for two of the 4 parton momenta $p_i, i = 1, 2, 3, 4$. This slicing procedure with an invariant mass cut is most convenient for analytical calculations. The integration over only one of the invariants is possible only when the singular contributions have been separated. To achieve this a partial fraction decomposition of the 4-parton matrix elements is carried out (see [22] for details). Then the EEC function is calculated from three separate contributions:

(a) The first contribution contains the singular parts of the partial fractioned 4-parton matrix elements integrated over one invariant inside the slicing cut y_{min} together with the virtual corrections to the $q\bar{q}g$ final state. This contribution corresponds to the term $F(0) \ln y_{min}$ in (8) for the example integral and depends strongly on y_{min} with the dominant term $\propto (-\ln^2 y_{min})$.

(b) The second contribution contains the remaining non-singular part of the 4-parton matrix elements which is the difference between the full 4-parton matrix element and the singular part already included in (a) integrated over the same region as in (a). This part corresponds obviously to the term T_f in (8).

(c) The third part consists of all contributions outside the singular region (a), i.e. with the integration over $y_{ij} > y_{min}$, which is computed numerically with $\cos \chi$ given by (9) with $i, j = 1, 2, 3, 4$. This part represents the first term in the example integral on the right-hand side of (8).

The calculation of the 4-parton contributions needed in (a) proceeds as follows. First the cross section for $e^+e^- \rightarrow q\bar{q}gg$ (the $q\bar{q}q\bar{q}$ final state is less singular and does not require partial fractioning; otherwise it is treated similarly) has the general form

$$d^5\sigma = \left(\frac{\alpha_s}{2\pi}\right)^2 f(y_{ij}) dPS^{(4)}. \quad (12)$$

The right-hand side of (12) has pole terms proportional to $y_{ij}^{-1}, (ij = 13, 14, 23, 24, 34)$ which are separated by the partial fractioning. For example, the contribution proportional to the colour factor C_F^2 has the structure

$$f(y_{ij}) = \frac{A_{13}}{y_{13}} + (1 \leftrightarrow 2) + (3 \leftrightarrow 4) + (1 \leftrightarrow 2, 3 \leftrightarrow 4) \quad (13)$$

where the momentum labels are $1, 2, 3, 4 = q, \bar{q}, g, g$. The terms proportional to y_{13}^{-1} and y_{14}^{-1} , respectively y_{23}^{-1} and y_{24}^{-1} , become singular when one of the gluons is infrared or collinear with the quark, respectively antiquark. They produce the dominant negative contributions to $B(\chi)$ after integration over the unresolved regions $y_{13} < y_{min}$, $y_{23} < y_{min}$, etc. when they are added to the virtual contributions. This integration is done only for one of the four terms in (13) which are related by permutation of the momentum labels. It is important to note that with

this procedure of slicing we do not calculate genuine 3-jet cross sections since only one of the pairings ij of two partons is recombined into one jet in the first, second etc. term in (13). The four terms in (13) are separated into singular and non-singular terms. The singular terms are regularized by dimensional regularization. The singularities in ϵ after integration compensate against the singularities in the $O(\alpha_s^2)$ one-loop corrections to $e^+e^- \rightarrow q\bar{q}g$. The result from the contribution (a) will be denoted the singular contribution, abbreviated by **sing** in the figures and tables which contain our results.

The other two contributions (b) and (c) come exclusively from the 4-parton tree diagrams. The part (b) consists of the non-singular terms in A_{13}/y_{13} etc. in (13) which are also integrated up to the cutoff. They do not participate in the cancellation of the infrared/collinear singularities between tree and virtual diagrams. The third part (c) is connected with the contribution above the slicing cut, $y_{13} > y_{min}$ (in the first term of (13)), which is computed numerically. It is important to note that the same expression for $f(y_{ij})$ with partial fractioning is used as in the singular region and that the integration up to y_{min} over y_{13} is applied only to the first term in (13). In the other terms the integration is over the variables y_{23}, y_{14} and y_{24} . The partial fractioning is not unique in the sense that non-singular terms can be distributed between the terms proportional to A_{ij} in (13). In the figures and tables and in the discussion below the contributions (b) and (c) will be called finite terms (**fin**) and real terms (**real**), respectively.

To proceed with the calculation we must specify the singular contributions given by A_{ij}/y_{ij} in (13). These singular terms factorize into the pole terms y_{ij}^{-1} times a factor which can be identified with the LO matrix element for $e^+e^- \rightarrow q\bar{q}g$. Only because of this factorization one is able to perform the cancellation with the virtual contributions. The identification of this factor with the LO matrix element amounts to specifying combinations of the 4-parton kinematic variables for the $q\bar{q}gg$ final state which define a 3-jet final state. These 3 jets can then be identified with the 3 partons of the LO matrix element. Usually this is done with the help of invariants built from the momenta of the $q\bar{q}gg$ final state. For example in the ERT approach [11] which was followed in all the calculations using the subtraction method, the relation was such, that in the pole term proportional to y_{ij}^{-1} the 3-jet variables are y_{134}, y_{24} and y_{123} ($y_{ijk} = (p_i + p_j + p_k)^2/s$). For three massless jets one has $y_{134} + y_{24} + y_{123} = 1$. This agrees with the 4-parton energy-momentum relation $y_{134} + y_{24} + y_{123} - y_{13} = 1$ only in the limit $y_{13} \rightarrow 0$. Therefore in [22] two other schemes have been considered: (1) the so-called KL scheme where y_{134}, y_{24} and $y_{123} - y_{13}$ are used instead; (2) the so-called KL' scheme, where the 3-jet variables are $y_{134}, y_{24} - y_{13}$ and y_{123} . Of course there are many more possibilities. This non-uniqueness of the definition of 3-jet variables for a 4-parton final state can not be avoided if one wants to cancel the infrared and collinear singularities between real and virtual contributions before the distribution in the final observable, i.e., in our case, in $\cos \chi$, is computed. This difference in the 3-jet variables is supposed to have no effect for $y_{min} \rightarrow 0$, i.e. in this limit we expect no difference in the results for the KL, KL' and ERT scheme. Since y_{min} is really never put equal to zero we must anticipate an effect from these different schemes in practice. From this discussion it is clear that in the calculation of the EEC function there is an ambiguity which is not visible in the simplified example integral discussed in the introduction. There, $F(0)$ can be defined uniquely: since F depends only on one variable, $F(0)$ is the residue of the pole. With more than one variable, however, the equivalent of $F(0)$ depends on which of the other variables are kept fixed and identified as 3-jet variables.

In the following we present separate results for the contributions of the C_F^2 , $C_F N_C$ and $C_F N_f$ parts of $B(\chi)$ as defined in (10), where we include the colour factor, i.e. we plot $\sin^2 \chi C_F^2 B_{C_F}(\chi)$ etc. for the three contributions **sing**, **fin** and **real** for a slicing cut $y_{min} = 10^{-4}$. We have chosen the KL' scheme for these plots and factored out $\sin^2 \chi$ to be able to plot with a linear scale. In Fig. 1 we have plotted the contributions for the C_F^2 part as a function of $\cos \chi$. We see that the real part is large and positive whereas the singular part is large and negative as we expect. The sum of both terms is small and negative for $\cos \chi \rightarrow \pm 1$, since the singular terms $\propto \ln^n y_{min}$, $n = 1, 2$, cancel in the sum. The finite term (**fin**) is very small. In the figure it is hard to distinguish it from the zero line. The same plot for the $C_F N_C$ part is seen in Fig. 2. Here we have two classes of pole terms coming either from the $qg(\bar{q}g)$ or the gg recombination. The corresponding real and non-singular parts are denoted **real**(13), **fin**(13) and **real**(34), **fin**(34), respectively. In the singular term both contributions (13) and (34) are added together for convenience. We see that the **fin**(34) is larger than **fin**(13) and **real**(34) (**real**(13)) is large positive (large negative). The total sum is positive. For the $C_F N_f$ contribution, calculated for $N_f = 5$ and exhibited in Fig. 3, we have only the singular and the real contributions. The finite terms are included already in the singular terms (see [22] for details). The singular and the real contributions contain terms which are proportional to $(-\ln y_{min})$ and $\ln y_{min}$, respectively. These terms cancel in the sum which is negative and smaller. In addition we have plotted the contribution of the $q\bar{q}q\bar{q}$ interference term. This term is actually proportional to $C_F(C_F - N_C/2)$ and should be distributed to the C_F^2 and $C_F N_C$ terms. For convenience we have included it here. Since it has no singularities it can be calculated numerically without difficulties. Its contribution is very small and negligible compared to the other terms. The sum in Fig. 3 includes this interference term, i.e. the sum contains all 4-quark contributions. In Fig. 4 the C_F^2 , $C_F N_C$ and the $C_F N_f$ contributions are plotted together with the sum of all three colour terms. We see that the $C_F N_C$ term is the most important one and it is positive. The $C_F N_f$ term is smaller and negative. The C_F^2 term is less important. The sum is essentially given by the sum of the $C_F N_C$ and the $C_F N_f$ parts except near the wings of the EEC distribution. The corresponding curves for the KL scheme look similar and will not be shown here. For larger y_{min} values the results change. For the KL' scheme the EEC correlation function decreases with increasing y_{min} . For the KL scheme this decrease occurs in particular for the wings of the NLO EEC function.

To obtain an overview of the most interesting central region we give the numbers in Tab. 1 for $\cos \chi = 0$ and $y_{min} = 10^{-k}$, $k = 2, 3, 4, 5, 6$. Since the numerical results fluctuate from bin to bin we have made a polynomial fit to our results in the interval $-0.40 < \cos \chi < 0.40$ and quote the result of this fit at $\cos \chi = 0$. We give the results for the different colour factors. We see that the $C_F N_f$ term is independent of y_{min} , which we expect because of the less singular behaviour of this part. The variation of the EEC function results in particular from the variation of the C_F^2 term, whereas the variation of the $C_F N_C$ contribution with y_{min} is much smaller. In the KL case the variation of the C_F^2 contribution is smaller, so that also the total sum is fairly constant. The splitting up of $B(\chi)$ into the contributions from the various regions for $\cos \chi = 0$ and $y_{min} = 10^{-4}$ is given in Tab. 2 for the KL' case. We see that the finite part **fin**(34) is still not negligible for this slicing cut. It is still more than 10% of the total sum and larger than the absolute value of the total C_F^2 contribution. The dependence of this particular contribution on the value of the slicing cut is shown in Fig. 5. The $q\bar{q}q\bar{q}$ interference term is negligible and much smaller than the total error.

Results for the pure phase space slicing method can be obtained by subtracting the contributions of the finite terms from the results in Tab. 1. The resulting numbers for the same y_{min} as in Tab. 1 are collected in Tab. 3, again for the different colour factors and the KL' and KL schemes. We see that the convergence with y_{min} is slower than for the hybrid method. The slow convergence comes mostly from neglecting the term `fin(34)` which is the largest one of all the finite contributions (see Tab. 2). Even for the larger y_{min} values the results for the KL' and KL approaches differ very little. The difference between the two schemes in Tab. 1 comes essentially from the finite term in the C_F^2 contribution which changes stronger with y_{min} in the KL' scheme. The slower convergence of the pure phase space slicing method was also observed by Glover and Sutton [9]. If we compare the results for the hybrid and the phase space slicing method at $y_{min} = 10^{-6}$ we see that they agree inside the numerical errors. The difference of $B(\chi = \pi/2)$, however, is still 1.15. This comes essentially from the term `fin(34)` which decreases very slowly with decreasing y_{min} , but is still non-negligible. In the calculation we obtained `fin(34)` = 1.154 ± 0.006 for both the KL' and the KL case. So, even with a slicing cut as small as 10^{-6} the finite parts are still not very small and produce an error of approximately 2% for $B(\chi = \pi/2)$ if one uses the pure phase space slicing method. At $y_{min} = 10^{-5}$ the $B(\chi)$ differ already outside the given error. Thus, to obtain good values for the NLO coefficient $B(\chi)$ with the phase space slicing method one must go to extremely small y_{min} of the order of 10^{-6} or smaller. The dependence of $B(\chi = \pi/2)$ on y_{min} is shown in Fig. 6 for the hybrid and space space slicing method and for the KL' and KL scheme separately for y_{min} between 10^{-6} and 10^{-2} . We observe that there is little difference between the KL' and the KL scheme in the case of the phase space slicing procedure since these two schemes differ essentially only in the finite parts. For the phase space slicing method, $B(\chi = \pi/2)$ increases monotonically with decreasing y_{min} . With the hybrid method $B(\chi)$ first increases to a maximum near $y_{min} = 10^{-3}$ and then decreases towards the final value at $y_{min} = 10^{-6}$. For $y_{min} \leq 10^{-4}$ the two schemes, KL' and KL, give the same results inside the errors. We consider the value at $y_{min} = 10^{-6}$ which is $B(\chi = \pi/2) = 50.1 \pm 0.9$ as our final value. In Fig. 7 we have plotted $B(\chi)$ as a function of χ in the range $-0.96 < \cos \chi < 0.96$ for the same y_{min} for KL', as well as the result for $y_{min} = 10^{-4}$.

3 Comparison with other Results

In this section we compare with the results of previous calculations. Such a comparison was done already by Glover and Sutton who compared their results with those of AB, RSE, FK and KN. Therefore we can restrict ourselves to a comparison with the most recent evaluations, namely those of KN, GS and CE. It turns out that our results agree with those of KN and GS but not with the results of CE. Kunszt and Nason [8] calculated $B(\chi)$ with the subtraction method by reorganizing the ERT matrix elements to give numerically stable results. Glover and Sutton [9] determined $B(\chi)$ with all three methods, subtraction, phase space slicing and hybrid method. For the evaluation with the subtraction method they used the ERT matrix elements as given in the original work [11]. For the phase space slicing and the hybrid method they have constructed a completely independent program based on [24] but using squared matrix elements rather than helicity amplitudes as in [24]. Our calculation is based on the work reported in [22] which was developed independently of all the earlier results and which relied on the introduction of a slicing cut to isolate the infrared and collinear divergences. A further important ingredient was the use of partial fractioning in all invariants y_{ij} which lead to singularities so that only for one of these variables a slicing cut had to be introduced. We believe

that a similar technique was employed by Kunszt and Nason and by Glover and Sutton in their calculations.

In Fig. 6 we can see that at larger y_{min} the results vary with y_{min} , independently of the method that was used; even for $y_{min} < 10^{-5}$ we still have a non-negligible variation. Since on the other hand Glover and Sutton give explicit numerical results only for $y_{min} = 10^{-5}$ we have selected our results for the same y_{min} to perform the comparison. Since our calculational methods and those of Glover and Sutton are not the same, there is actually no reason that the two results should be identical for this particular y_{min} ; however, we believe that a comparison at the same y_{min} is more sensible than performing the comparison at different values. Since Kunszt and Nason used the subtraction method, there is no cut dependence in their results.

The comparison of our results with the results of these two groups is collected in Table 4. We see that we have perfect agreement. In particular our hybrid results agree very well with those of Glover and Sutton inside their respective errors (compare $KS^{(5)}, KS^{(6)}$ with $GS^{(4)}$). Concerning the phase space slicing method there is a small difference with GS outside the errors (compare $KS^{(7)}, KS^{(8)}$ with $GS^{(3)}$). Knowing that the finite parts are still non-negligible at $y_{min} = 10^{-5}$, we can not expect perfect agreement in this case.

Another important check between the various results is the decomposition of $B(\chi)$ into contributions for different colour factors. In Tables 1 and 3 we have given these contributions already for $B(\chi)$ at $\chi = \pi/2$. Equivalent results are not available from the publications in refs. [8, 9]. After their publication, Glover and Sutton calculated the contributions for the different colour factors for a comparison with the results of Clay and Ellis. Their results for $B(\chi = \pi/2)$ [25] are:

$$\begin{aligned} C_F^2 B_{C_F} &= -2.42 \pm 0.92, \\ C_F N_C B_{N_C} &= 77.20 \pm 2.08, \\ C_F N_f B_{N_f} &= -24.97 \pm 0.53. \end{aligned} \tag{14}$$

The sum of these terms is 49.8 ± 2.3 . By comparing with our results in Table 1 or Table 3 we observe perfect agreement of our colour decomposition with the Glover and Sutton results given above.

Concerning the more recent results of Clay and Ellis [10] there is no agreement with our results and with those of Kunszt-Nason or Glover-Sutton, respectively. From Fig. 1 of the Clay-Ellis paper we read off a value of about 57.0 for $B(\chi = \pi/2)$. The actual precision of their numerical results is 0.3% as stated by the authors. So, our value of B as well as that of KN or of GS differ by approximately 15% which can not be explained by numerical uncertainties in any one of the calculations. In our case the error is below 2% (for $y_{min} = 10^{-6}$). The difference is in the contributions with the colour factors C_F^2 and $C_F N_C$, since concerning B_{N_f} Clay and Ellis and Glover and Sutton achieved agreement [10]. It is clear that the $C_F N_f$ term is less problematic since the contributions to this term are less singular than those to the C_F^2 and $C_F N_C$ terms. The origin of the disagreement is unclear. Unfortunately we could not study this further, since Clay and Ellis have not explained the details of their calculation.

With respect to the earlier calculations of AB [5], RSE [4] and FK [7] we made some effort to understand the differences with these earlier results. The calculations of FK were done with

the phase space slicing method with $y_{min} = 10^{-4}$ and with the important difference that the real contributions are calculated with cuts $y_{ij} \geq 10^{-4}$ applied to all invariants of the 4-parton momenta. This was necessary since for the real contributions partial fractioning as in (13) was not performed. We found out, however, that for $y_{min} = 10^{-4}$ these additional cuts have a non-negligible effect when we apply them to the partial fractioned real term as given, for example, in (13). In the present calculation we used cuts only for those variables which are singular in the first, second etc. terms in (13). In [7] the reduction of the non-singular terms through these additional cuts was compensated by additional terms in the singular contributions, but presumably not fully. In the moment it is unclear, whether with much smaller cut values than 10^{-4} the method used by FK would give the same results as the present calculation. From the results given by FK it is clear that $y_{min} = 10^{-4}$ is not sufficiently small to obtain correct results. Furthermore, from Tables 1 and 3 we see that at $y_{min} = 10^{-4}$ there is already a difference of $\Delta B(\chi = \pi/2) = 6.03$ and 6.45 for the KL' and KL schemes, respectively, between the hybrid and the phase space slicing method. The results of AB [5] and RSE [4] are obtained with the subtraction method and therefore should agree with the results of KN and GS using the same method. We suspect that in these older calculations the so-called finite pieces (see (5)) are calculated also with cuts on all invariants y_{ij} in the 4-parton term (first term in (5)). In the work of Ali and Barreiro (first reference of [5]) such a cut $y_{ij} \geq 10^{-7}$ is explicitly stated and this cut was also used in the second paper [5, 26]. Concerning RSE we have no information on this point. If the interpretation that the additional cuts in AB and RSE are responsible for the reduction of their results is correct, it would mean that, similar as we observed for the FK calculation, one would need even smaller cuts below 10^{-7} to achieve convergence.

We also compared the EEC coefficient $B(\chi)$ for the other angles as shown in Fig. 7 with the results of Kunszt and Nason and found good agreement. We therefore conclude that the KN calculation gives the correct NLO coefficient $B(\chi)$. The older results RSE, AB and FK should be disregarded and not be used for a determination of α_s . If for the time being we also leave aside the results of Clay and Ellis [10] since their result has not been confirmed by other calculations, the theoretical error on α_s mentioned in the introduction can be eliminated. Then the SLD analysis [2] yields the following value for α_s from the measurement of the EEC:

$$\alpha_s(M_Z^2) = 0.125_{-0.003}^{+0.002}(\text{exp}) \pm 0.012(\text{theory}). \quad (15)$$

This agrees completely with the conclusion of Glover and Sutton [9]. Now the theoretical error comes exclusively from the scale change which in the SLD work [2] originates from a rather large variation with a scale factor f in the interval $0.002 \leq f \leq 4$.

In conclusion, motivated by the recent results of Clay and Ellis which disagreed with the earlier results of KN and GS, we have reevaluated the EEC using a completely independent approach which allowed us to obtain results for the phase space slicing and the hybrid method. The pure phase space slicing method needs extremely small slicing cuts, smaller than 10^{-6} , in order to achieve a good accuracy below 2%. This is due to the finite terms which converge very slowly to zero with decreasing cut. This shows that configurations with extremely small invariant masses can contribute to the EEC at all angles, i.e. also at angles far away from the two-jet region at $\chi \simeq \pi$. In our opinion the results of the older calculations seem to suffer from a too large slicing cut (FK) or from additional cuts in the evaluation using the subtraction method (RSE, AB) and therefore could yield only estimates of $B(\chi)$.

Acknowledgements

We thank E. Glover for communicating his results on the colour decomposition and A. Ali for useful discussions on his work with F. Barreiro.

Table Caption

- Tab. 1: NLO coefficient $B(\chi)$ at $\cos \chi = 0$ for various y_{min} and colour contributions in the KL' and KL scheme using the hybrid method.
- Tab. 2: Contribution to the NLO coefficient $B(\chi)$ at $\cos \chi = 0$ for $y_{min} = 10^{-4}$ for different colour factors from the regions `sing`, `real` and `fin` with the hybrid method and KL' scheme.
- Tab. 3: Same as in Table 1 with the phase space slicing method.
- Tab. 4: NLO coefficient $B(\chi)$ at $\cos \chi = 0$ for different calculations; (1) Table 3 of [8], (2) subtraction method, (3) phase space slicing method, $y_{min} = 10^{-5}$, (4) hybrid method, $y_{min} = 10^{-5}$ of ref. [9], (5) and (6) phase space slicing method for KL' and KL scheme from Table 3, (7) and (8) hybrid method for KL' and KL scheme from Table 1 ($y_{min} = 10^{-5}$).

Figure Caption

- Fig. 1: C_F^2 contributions to the NLO coefficient $\sin^2 \chi B(\chi)$ as a function of $\cos \chi$ for $y_{min} = 10^{-4}$ in the KL' scheme. Long-dashed line: singular contribution, short-dashed line: real contribution, dotted line: finite contribution. Full line: sum of all C_F^2 contributions.
- Fig. 2: $C_F N_C$ contributions to the NLO coefficient $\sin^2 \chi B(\chi)$ as a function of $\cos \chi$ for $y_{min} = 10^{-4}$ in the KL' scheme. Long-dashed line: singular contribution; real contributions: short-dashed: `real(13)`, dotted: `real(34)`; finite contributions: long dashed-dotted: `fin(13)`, short dashed-dotted: `fin(34)`; full line: sum of all $C_F N_C$ contributions.
- Fig. 3: 4-quark contributions to the NLO coefficient $\sin^2 \chi B(\chi)$ as a function of $\cos \chi$ for $y_{min} = 10^{-4}$ in the KL' scheme. Long-dashed line: singular contribution, dotted line: real contribution; short-dashed line: 4-quark interference contribution. Full line: sum of all 4-quark contributions.
- Fig. 4: Colour decomposition of the NLO coefficient $\sin^2 \chi B(\chi)$ as a function of $\cos \chi$ for $y_{min} = 10^{-4}$ in the KL' scheme. Long-dashed line: C_F^2 contribution, short-dashed line: $C_F N_C$ contribution, dotted line: $C_F N_f$ contribution; full line: sum of all contributions.

- Fig. 5: y_{min} dependence of $C_F N_C$ -**fin**(34) contribution to the NLO coefficient $B(\chi = \pi/2)$.
- Fig. 6: y_{min} dependence of the NLO coefficient $B(\chi = \pi/2)$. Upper curves are for the hybrid method, lower curves for the pure phase space slicing method. The two curves in each set are for the KL' and the KL scheme.
- Fig. 7: The complete NLO coefficient $B(\chi)$ as a function of $\cos \chi$ obtained with the hybrid method in the KL' scheme for $y_{min} = 10^{-4}$ (histogram) and $y_{min} = 10^{-6}$ (points with error bars).

References

- [1] P. Abreu et al., DELPHI Collaboration, Phys. Lett. B252 (1990) 149, Z. Phys. C59 (1993) 21;
M. Akrawy et al., OPAL Collaboration, Phys. Lett. B252 (1990) 159, ibid. B276 (1992) 547;
B. Adeva et al., L3 Collaboration, Phys. Lett. B257 (1991) 469, O. Adriani et al., L3 Collaboration, Phys. Lett. B284 (1992) 471.
- [2] K. Abe et al., SLD Collaboration, Phys. Rev. D50 (1994) 5580, ibid. D51 (1995) 962.
- [3] C. L. Basham, L. S. Brown, S. D. Ellis, T. S. Love, Phys. Rev. Lett. 41 (1978) 1585, Phys. Rev. D17 (1982) 2298.
- [4] D. G. Richards, W. J. Stirling, S. D. Ellis, Phys. Lett. 119B (1982) 193, Nucl. Phys. B229 (1983) 317.
- [5] A. Ali, F. Barreiro, Phys. Lett. 118B (1982) 115, Nucl. Phys. B286 (1984) 269.
- [6] H. N. Schneider, G. Kramer, G. Schierholz, Z. Phys. C22 (1984) 235.
- [7] N. K. Falck, G. Kramer, Z. Phys. C42 (1989) 459.
- [8] Z. Kunszt, P. Nason, G. Marchisini, B. R. Webber in "Z Physics at LEP 1" CERN 89-08, Vol. 1, eds. G. Altarelli, R. Kleiss and C. Verzegnassi (CERN, Geneva, 1989).
- [9] E. W. N. Glover, M. R. Sutton, Phys. Lett. B342 (1995) 375.
- [10] K. A. Clay, S. D. Ellis, Phys. Rev. Lett. 74 (1995) 4392.
- [11] R. K. Ellis, D. A. Ross, A. E. Terrano, Nucl. Phys. B178 (1981) 421.
- [12] K. Abe et al., SLD Collaboration, Phys. Rev. D52 (1995) 4240.
- [13] K. Fabricius, G. Kramer, I. Schmitt, G. Schierholz, Z. Phys. C11 (1982) 315.
- [14] Z. Kunszt, D. E. Soper, Phys. Rev. D46 (1992) 196.
- [15] K. Fabricius, I. Schmitt, G. Schierholz, G. Kramer, Phys. Lett. 97B (1980) 431.
- [16] F. Gutbrod, G. Kramer, G. Schierholz, Z. Phys. C21 (1984) 235.
- [17] R. K. Ellis, D. A. Ross, Phys. Lett. 106B (1981) 88.
- [18] Z. Kunszt, Phys. Lett. 107B (1981) 123.
- [19] D. Decamp et al., ALEPH Collaboration, Phys. Lett. B257 (1991) 479.
- [20] G. Kramer, H. Spiesberger, Desy report, DESY 95-097 (May 1995), Z. Phys. C (to be published).
- [21] S. D. Ellis, W. J. Stirling, Phys. Rev. D23 (1981) 214; S. D. Ellis, N. Fleishon, W. J. Stirling, Phys. Rev. D24 (1981) 1386;
J. C. Collins, D. E. Soper, Nucl. Phys. B193 (1981) 381, ibid. B197 (1982) 446, ibid. B213 (1983) 545, ibid. B284 (1987) 253.

- [22] G. Kramer, B. Lampe, Fortschr. Phys. 37 (1989) 161.
- [23] A. Ali et al., Phys. Lett. 82B (1979) 285, Nucl. Phys. B167 (1980) 454.
- [24] W. T. Giele, E. W. N. Glover, Phys. Rev. D46 (1992) 1980.
- [25] E. W. N. Glover (private communication).
- [26] A. Ali (private communication).

Table 1:

NLO Coefficient $B(\chi)$ for $\cos \chi = 0$					
y_{min}	method	C_F^2	$C_F N_C$	$C_F N_f$	sum
10^{-6}	KL'	-2.68 ± 0.68	78.16 ± 0.60	-25.388 ± 0.071	50.11 ± 0.91
	KL	-2.57 ± 0.68	78.03 ± 0.60	-25.388 ± 0.071	50.09 ± 0.91
10^{-5}	KL'	-2.09 ± 0.44	79.22 ± 0.36	-25.159 ± 0.055	51.96 ± 0.58
	KL	-2.02 ± 0.44	79.12 ± 0.36	-25.159 ± 0.055	51.87 ± 0.58
10^{-4}	KL'	-2.18 ± 0.26	80.81 ± 0.19	-25.116 ± 0.041	53.52 ± 0.32
	KL	-1.83 ± 0.26	80.87 ± 0.19	-25.116 ± 0.041	53.93 ± 0.32
10^{-3}	KL'	-3.77 ± 0.13	81.621 ± 0.092	-24.965 ± 0.026	52.88 ± 0.16
	KL	-1.61 ± 0.13	81.575 ± 0.093	-24.965 ± 0.026	55.00 ± 0.16
10^{-2}	KL'	-11.082 ± 0.054	80.309 ± 0.063	-24.759 ± 0.015	44.465 ± 0.084
	KL	-2.302 ± 0.046	79.838 ± 0.065	-24.759 ± 0.015	52.566 ± 0.086

Table 2:

NLO Coefficient $B(\chi)$ for $\cos \chi = 0$, $y_{min} = 10^{-4}$		
colour factor	region	$B(\cos \chi = 0)$
C_F^2	sing	-410.18 ± 0.16
	real	408.36 ± 0.020
	fin	-0.3744 ± 0.0019
	sum	-2.18 ± 0.26
$C_F N_C$	sing	-68.818 ± 0.071
	real(13)	-120.62 ± 0.12
	real(34)	263.80 ± 0.12
	fin(13)	-0.3023 ± 0.0007
	fin(34)	6.706 ± 0.016
	sum	80.81 ± 0.19
$C_F N_f$	sing	-44.349 ± 0.018
	real	19.227 ± 0.037
	sum	-25.116 ± 0.041
$C_F^2 - C_F N_C / 2$	$(q\bar{q})_{int}$	-0.0851 ± 0.0004
sum	sum	53.52 ± 0.32

Table 3:

NLO Coefficient $B(\chi)$ for $\cos \chi = 0$					
y_{min}	<i>method</i>	C_F^2	$C_F N_C$	$C_F N_f$	<i>sum</i>
10^{-6}	KL'	-2.67 ± 0.68	77.02 ± 0.60	-25.388 ± 0.071	48.98 ± 0.91
	KL	-2.58 ± 0.68	76.90 ± 0.60	-25.388 ± 0.071	48.95 ± 0.91
10^{-5}	KL'	-2.03 ± 0.44	76.26 ± 0.35	-25.159 ± 0.055	49.06 ± 0.56
	KL	-2.04 ± 0.44	76.12 ± 0.35	-25.159 ± 0.055	48.92 ± 0.56
10^{-4}	KL'	-1.80 ± 0.26	74.39 ± 0.19	-25.116 ± 0.041	47.47 ± 0.32
	KL	-1.89 ± 0.26	74.48 ± 0.19	-25.116 ± 0.041	47.49 ± 0.32
10^{-3}	KL'	-1.73 ± 0.13	69.714 ± 0.086	-24.965 ± 0.026	43.02 ± 0.15
	KL	-1.86 ± 0.13	69.791 ± 0.087	-24.965 ± 0.026	42.97 ± 0.15
10^{-2}	KL'	-2.610 ± 0.046	63.751 ± 0.041	-24.759 ± 0.015	36.380 ± 0.063
	KL	-3.336 ± 0.049	63.887 ± 0.046	-24.759 ± 0.015	35.791 ± 0.068

Table 4:

NLO Coefficient $B(\chi)$ for $\cos \chi = 0$	
<i>calculation</i>	$B(\cos \chi = 0)$
$KN^{(1)}$	51.25 ± 2.67
$GS^{(2)}$	52.39 ± 0.83
$GS^{(3)}$	51.15 ± 0.68
$GS^{(4)}$	52.29 ± 2.08
$KS^{(5)}$	51.96 ± 0.58
$KS^{(6)}$	51.87 ± 0.58
$KS^{(7)}$	49.06 ± 0.56
$KS^{(8)}$	48.92 ± 0.56

Fig. 1

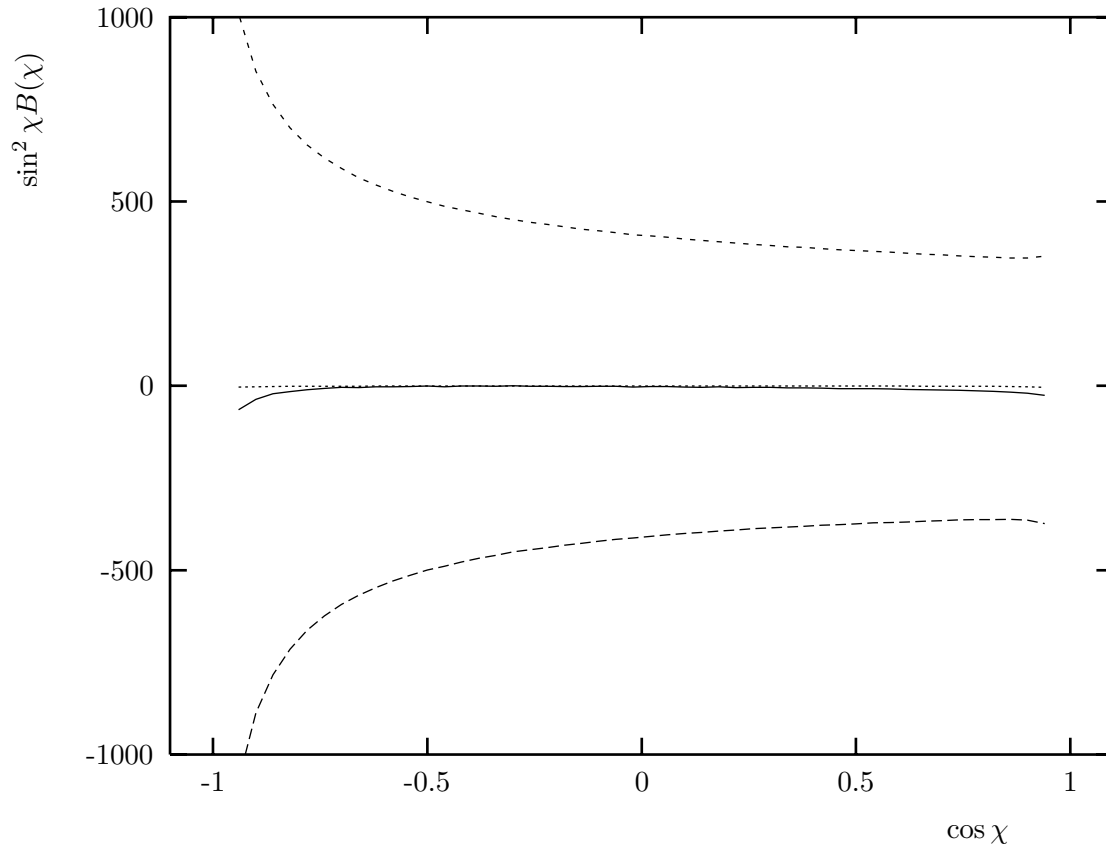


Fig. 2

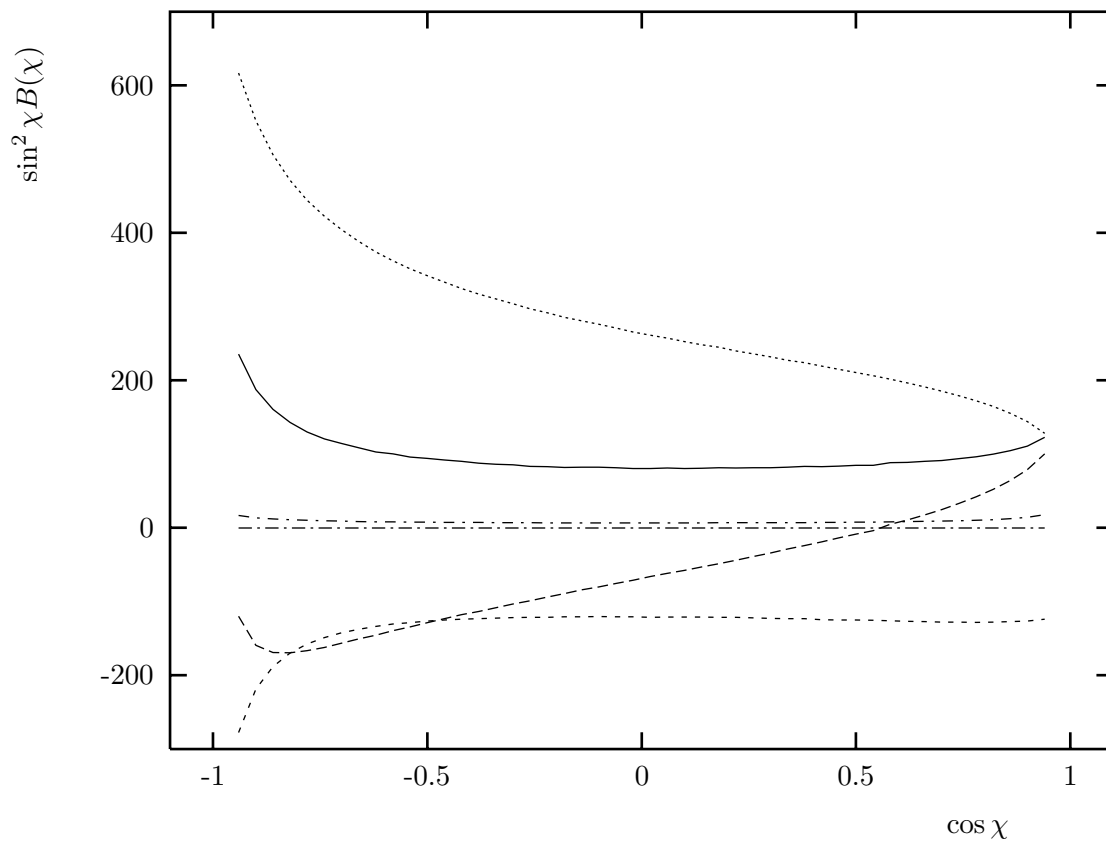


Fig. 3

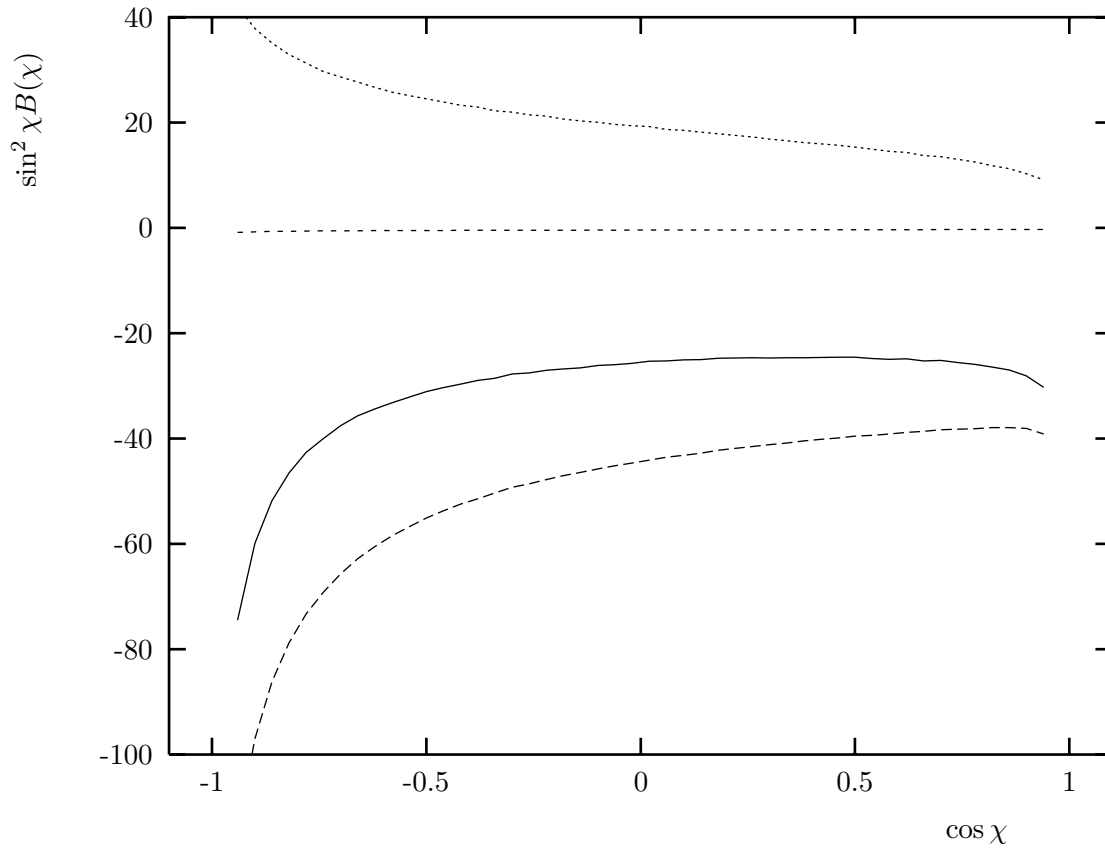


Fig. 4

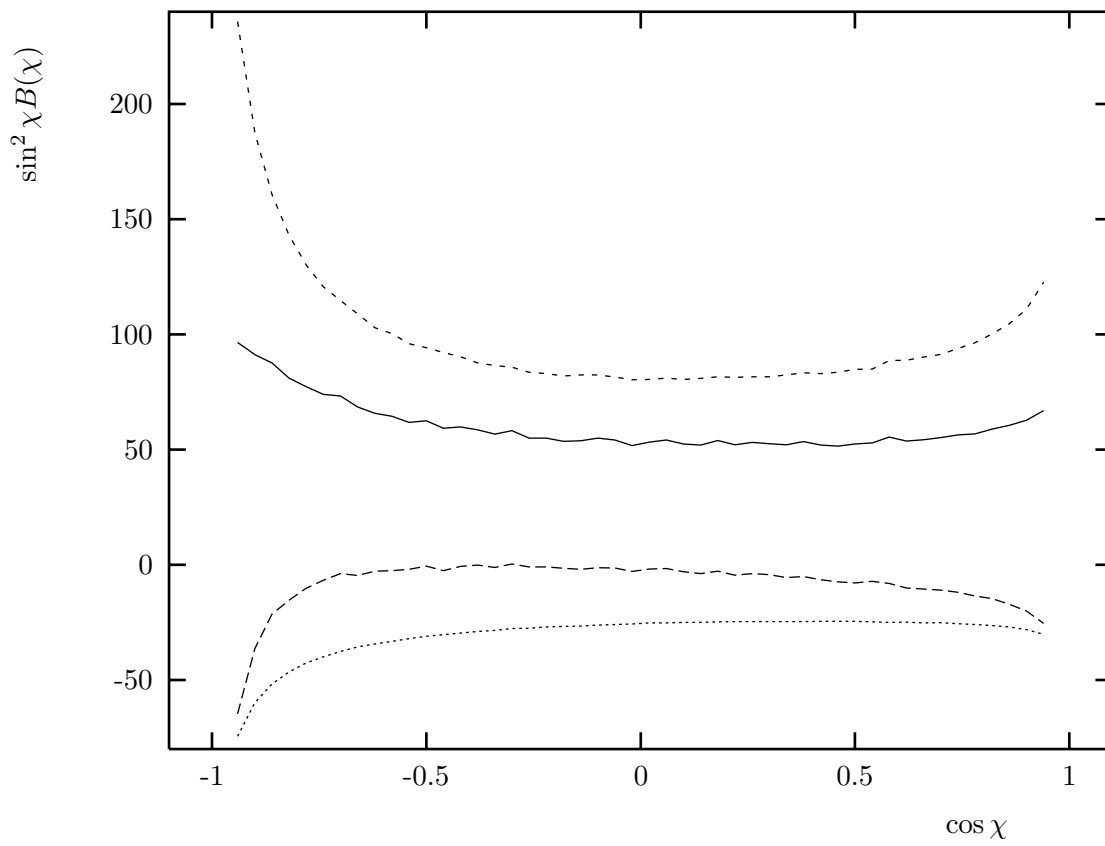


Fig. 5

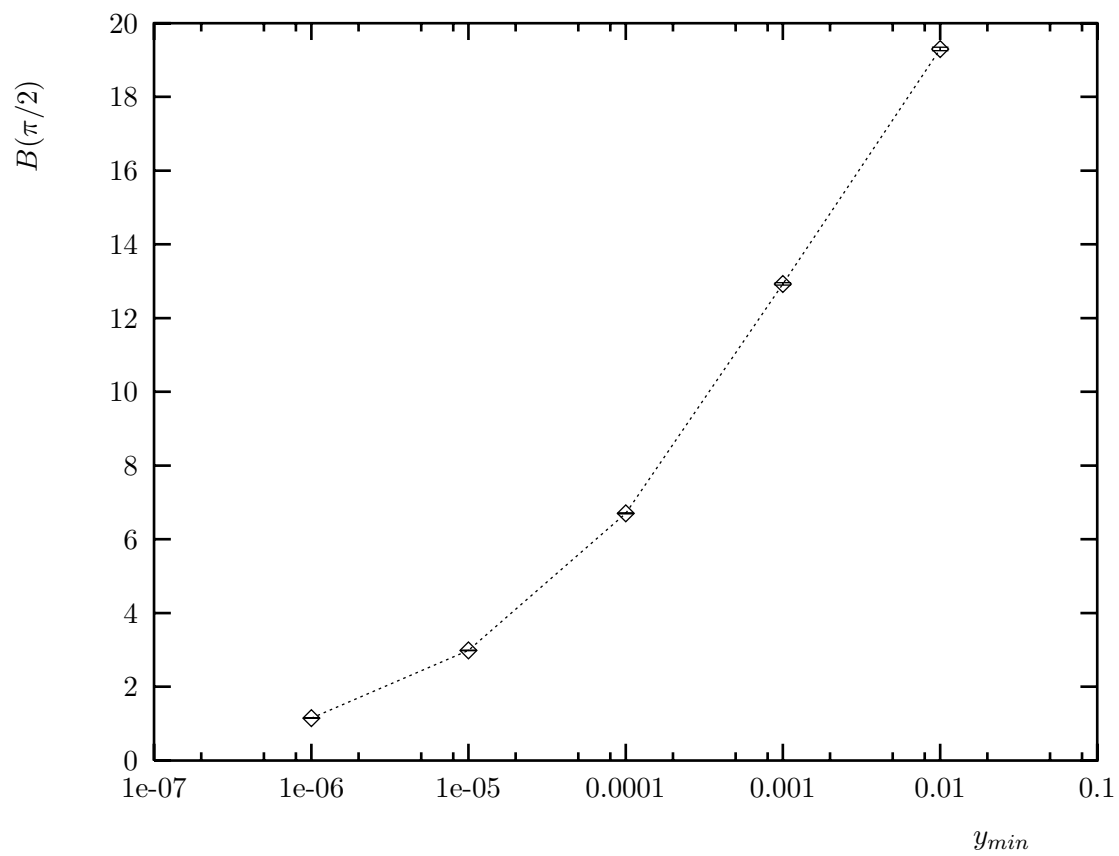


Fig. 6

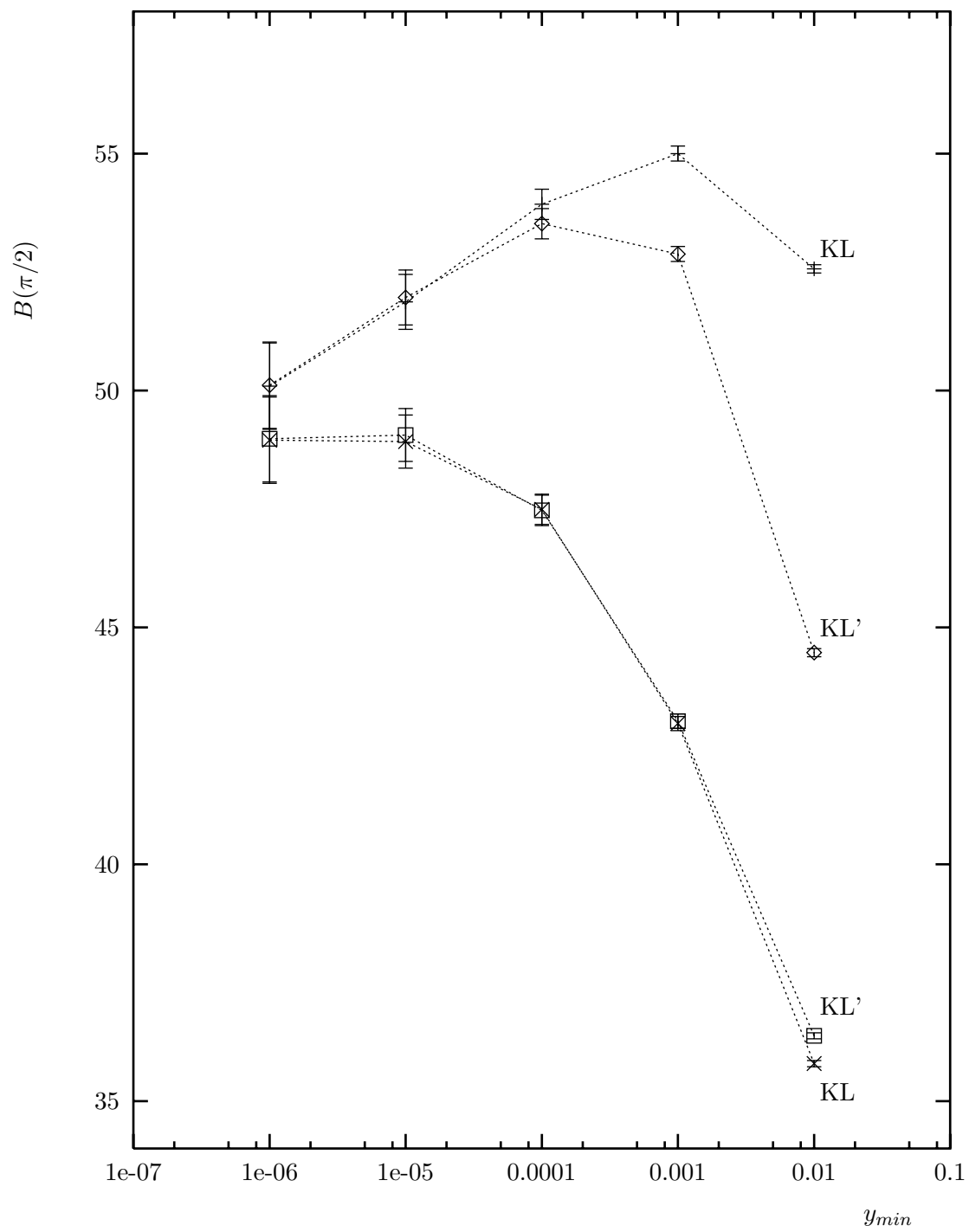


Fig. 7

